

Dynamic polarization potentials for the halo nucleus ${}^6\text{He}$ in medium-energy elastic scattering

B. Abu-Ibrahim^{1,2} and Y. Suzuki¹

¹*Department of Physics, Niigata University, Niigata 950-2181, Japan*

²*Department of Physics, Cairo University, Giza 12613, Egypt*

(Received 6 February 2004; published 16 July 2004)

We study dynamic polarization potentials for a halo nucleus ${}^6\text{He}$ scattered by a ${}^{12}\text{C}$ target in the eikonal approximation. We use a realistic, six-nucleon wave function of ${}^6\text{He}$ to include both the halo-neutron and the core-nucleon excitations on an equal footing. We discuss the energy dependence of the polarization potential in relation to that of the nucleon-target optical potential. The imaginary part of the polarization potential changes a sign (negative to positive with increasing energy) around the incident energy of 200 MeV/nucleon, which gives different contributions, depending on the energy, to the elastic differential cross section as well as the reaction cross section.

DOI: 10.1103/PhysRevC.70.011603

PACS number(s): 25.60.Bx, 11.80.Fv, 24.10.-i, 25.60.Dz

A halo nucleus is characterized by one or two weakly bound neutrons surrounding a core nucleus. The halo part extends to large distances beyond the radius of the core. This unusual structure offers a variety of new phenomena of keen interest. One of the important consequences is that the halo neutrons can easily be excited to continuum states. This implies that, in the scattering of the halo nucleus, virtual and/or actual excitations to the continuum states occur with high probability and as its result produces a strong effect on the optical potential for the halo nucleus. The deviation of a nucleus-nucleus optical potential from its folded potential, with the exchange due to the antisymmetrization between the nuclei being neglected, is called a dynamic polarization potential (DPP) [1]. The necessity of the DPP is in fact well known for weakly bound projectiles like ${}^6\text{Li}$ and ${}^7\text{Li}$ [2,3]. What is challenging is that the continuum states play a primary role as only a few or no bound excited states exist for the halo nucleus. The importance of the DPP has long been recognized in other fields such as atomic physics, where the dipole excitation to discrete states plays a key role to produce a long-range potential. Some progress on the dipole polarizability for halo nuclei has recently been made [4,5], but no systematic analysis for the DPP due to the nuclear force has been done yet.

The recent elastic differential cross section data of ${}^6\text{He} + {}^{12}\text{C}$ at 38.3 MeV/nucleon [6] has clearly shown the importance of the DPP. The DPP for ${}^6\text{Li}$ and ${}^7\text{Li}$ scatterings were successfully accounted for by continuum-discretized coupled-channels (CDCC) calculations [3], in which the excitation energy of the continuum state was relatively low. For the DPP of a halo nucleus, however, the excitation energy must be extended further, and moreover even the excitation of the core part may produce a sizable contribution to the DPP as the beam energy is usually around a few hundred MeV/nucleon. In fact we have analyzed the ${}^6\text{He} + {}^{12}\text{C}$ elastic scattering data in the eikonal approximation using a nucleon- ${}^{12}\text{C}$ optical potential as a basic input [7], and obtained a satisfactory fit [8] to the experiment by an *ab initio* calculation which employs a realistic ${}^6\text{He}$ wave function generated from a variational Monte Carlo method [9].

The purpose of this study is to assess the relative importance of the halo-neutron and core-nucleon excitations due to

the nuclear force in the elastic scattering at medium energies of 50–800 MeV/nucleon, to investigate their effects on the elastic scattering differential cross section and the reaction cross section, and to clarify the characteristics of the DPP in relation to the underlying nucleon-target potential. To achieve this goal, we can exploit the predictive power of the *ab initio* calculation which is free from energy-dependent, adjustable parameters. We expect that we can determine the range of validity of a CDCC calculation which assumes a rigid core. As a prototype of the analysis we consider the ${}^6\text{He} + {}^{12}\text{C}$ case because of the following reasons: ${}^6\text{He}$ is a well-known halo nucleus, the scattering data are available at 40 MeV/nucleon, the sophisticated wave functions which take into account various correlations such as short-range and tensor correlations are available for both ${}^6\text{He}$ and ${}^4\text{He}$ [9], and in addition a global p - ${}^{12}\text{C}$ optical potential [10] is available as a function of energy.

Let ψ_0 be the (translation-invariant) intrinsic wave function of the projectile's ground state. The projectile's wave function after colliding with the target is given in the eikonal approximation by

$$e^{i\sum_j \chi_{\text{NT}}(\mathbf{b}+s_j)} \psi_0, \quad (1)$$

where \mathbf{b} is the impact parameter perpendicular to the beam (z) direction and s_j is the projection onto the xy plane of the nucleon coordinate relative to the projectile's center-of-mass. In Eq. (1) χ_{NT} is the phase-shift function calculated from the nucleon-target optical potential V_{NT} :

$$\chi_{\text{NT}}(\mathbf{b}) = -\frac{1}{\hbar v} \int_{-\infty}^{\infty} dz V_{\text{NT}}(\mathbf{b} + z\hat{z}), \quad (2)$$

where v is the incident velocity of the projectile-target relative motion. The elastic scattering can be described in terms of the phase-shift function $\chi(\mathbf{b})$:

$$e^{i\chi(\mathbf{b})} = \langle \psi_0 | e^{i\sum_j \chi_{\text{NT}}(\mathbf{b}+s_j)} | \psi_0 \rangle. \quad (3)$$

This phase shift contains the effect of couplings to various inelastic channels including the continuum states. On the contrary, the phase shift, $\chi_{\text{f}}(\mathbf{b})$, corresponding to the folded potential, is given by $\chi_{\text{f}}(\mathbf{b}) = \langle \psi_0 | \sum_j \chi_{\text{NT}}(\mathbf{b}+s_j) | \psi_0 \rangle$ and con-

tains no coupling effect. Thus the phase shift responsible for the DPP, χ_{DPP} , is defined by $\chi_{\text{DPP}} = \chi - \chi_{\text{f}}$. A relationship between these various phase shifts and the corresponding potentials is the same as Eq. (2), and it is straightforward to invert the phase-shift function to obtain the potential [11]. This simple method appears to be suitable for our purpose as the inversion is consistent in the eikonal approximation. See, for example, Ref. [12] for other sophisticated inversion methods.

The matrix element of Eq. (3) contains a multidimensional integration over all the internal coordinates of the projectile nucleus. Being a formidable task, a real application of the formula has so far been severely limited in spite of the fact that the eikonal approximation is valid and acceptable at intermediate and high energies [13–15]. However, it is now possible to evaluate the phase-shift function accurately [16] even for sophisticated wave functions by Monte Carlo integration.

The DPP of ${}^6\text{He}$ contains the contributions of excitation and breakup processes of both the core and halo nucleons. As the core part of ${}^6\text{He}$ is considered approximately the same as ${}^4\text{He}$ [17], we may decompose the DPP phase-shift into two parts:

$$\chi_{\text{DPP}}({}^6\text{He}, \mathbf{b}) = \chi_{\text{DPP}}({}^4\text{He}, \mathbf{b}) + \chi_{\text{DPP}}(2n, \mathbf{b}). \quad (4)$$

The center of mass of the ${}^4\text{He}$ core actually fluctuates around that of ${}^6\text{He}$, so its impact parameter is not necessarily equal to \mathbf{b} but has some distribution around it. Here we simply assume that $\chi_{\text{DPP}}({}^4\text{He}, \mathbf{b})$ is given by $\chi({}^4\text{He}, \mathbf{b}) - \chi_{\text{f}}({}^4\text{He}, \mathbf{b})$ from the ${}^4\text{He}$ wave function. $\chi_{\text{DPP}}(2n)$ is defined by the difference, $\chi_{\text{DPP}}({}^6\text{He}) - \chi_{\text{DPP}}({}^4\text{He})$. The decomposition is thus model-dependent but appears reasonable for a qualitative estimate of each contribution. The full phase shift for ${}^6\text{He}$ is thus written as a sum of the folding term and the two DPP terms

$$\chi({}^6\text{He}, \mathbf{b}) = \chi_{\text{f}}({}^6\text{He}, \mathbf{b}) + \chi_{\text{DPP}}({}^4\text{He}, \mathbf{b}) + \chi_{\text{DPP}}(2n, \mathbf{b}). \quad (5)$$

As V_{NT} we use the central part of the global optical potential [10] unless otherwise stated, ignoring the difference between p - ${}^{12}\text{C}$ and n - ${}^{12}\text{C}$ interactions. This potential is determined by the Dirac phenomenology and gives a good fit to p - ${}^{12}\text{C}$ elastic scattering data. The incident energy *per nucleon*, E , considered in the present study covers 50, 100, 200, 400, and 800 MeV. The real part of V_{NT} changes its sign: It is attractive below 300 MeV with its depth decreasing as the energy increases, and becomes repulsive in its interior region above 300 MeV. The real part of the volume integral $J = \int d\mathbf{r} V_{\text{NT}}(r)/A$ (in units of MeV fm³) changes from -328 to 43 as E changes from 50 to 800 MeV. On the contrary, the imaginary part is always absorptive (negative) with its depth increasing as the energy increases. Reflecting that a pion production threshold for a nucleon incident on a nucleus is around 250 MeV, the depth of the imaginary potential becomes very large above that energy: The imaginary part of J changes only a little around -116 up to $E=200$ MeV but jumps to -242 and -374 at 400 and 800 MeV, respectively. It is noted that the energy-dependence of p - ${}^{40}\text{Ca}$ and p - ${}^{208}\text{Pb}$ optical potentials [10] is similar to that of p - ${}^{12}\text{C}$ except for 200 MeV.

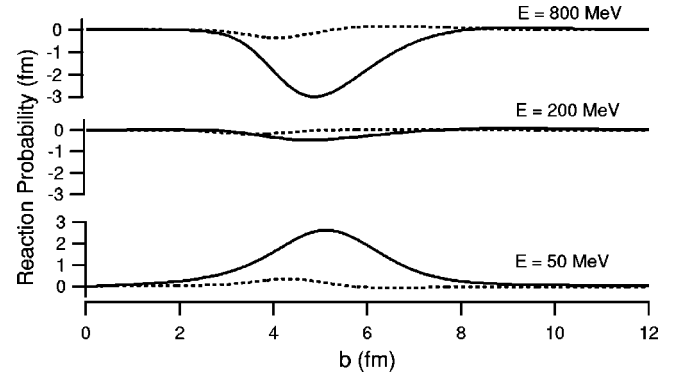


FIG. 1. The reaction probability of ${}^6\text{He}$ incident on ${}^{12}\text{C}$ as a function of the impact parameter. E is the bombarding energy per nucleon. The solid line corresponds to the halo-neutron excitation, and the dotted line to the ${}^4\text{He}$ -core excitation.

To see a qualitative feature of the DPP, we recall that the leading term of the DPP is given by [14]

$$\chi_{\text{DPP}}(\mathbf{b}) \approx \frac{i}{2} \langle \psi_0 | \left[\sum_j \chi_{\text{NT}}(\mathbf{b} + \mathbf{s}_j) - \chi_{\text{f}}(\mathbf{b}) \right]^2 | \psi_0 \rangle. \quad (6)$$

Thus χ_{DPP} is proportional to $(i/2)(V_0 + iW_0)^2 = -V_0W_0 + (i/2)(V_0^2 - W_0^2)$ if V_{NT} is assumed to be of form $(V_0 + iW_0)f(r)$. This simple argument suggests that the real (imaginary) part of the DPP has the same sign as V_0W_0 ($W_0^2 - V_0^2$). We will confirm later that this rule proves right. We do not use the above approximation but calculate the phase-shift function accurately in this paper.

We first discuss the reaction cross section, $\sigma_{\text{R}} = \int d\mathbf{b} (1 - |e^{i\chi(\mathbf{b})}|^2)$, of ${}^6\text{He}$ by decomposing the “reaction probability,” $1 - |e^{i\chi({}^6\text{He})}|^2$, into four terms:

$$\begin{aligned} 1 - |e^{i\chi({}^6\text{He})}|^2 &= (1 - P_{\text{f}}) + P_{\text{f}}(1 - |e^{i\chi_{\text{DPP}}(2n)}|^2) \\ &\quad + P_{\text{f}}(1 - |e^{i\chi_{\text{DPP}}({}^4\text{He})}|^2) \\ &\quad - P_{\text{f}}(1 - |e^{i\chi_{\text{DPP}}(2n)}|^2)(1 - |e^{i\chi_{\text{DPP}}({}^4\text{He})}|^2), \end{aligned} \quad (7)$$

where $P_{\text{f}} = |e^{i\chi_{\text{f}}({}^6\text{He})}|^2$ is the survival probability of the incident flux against the absorption of the folded potential. The reaction cross section calculated from the first term is called an optical-limit value σ_{f} . The above decomposition is made to emphasize the relative importance of the two DPP terms. Figure 1 shows the second and third terms, multiplied by $2\pi b$. The contribution of each term to σ_{R} is listed in Table I, which confirms that, aside from the leading σ_{f} term, the $2n$ -DPP term is a main contributor to σ_{R} but the other terms play a minor role. A remarkable point is that the $2n$ -DPP term gives a positive contribution to σ_{R} at lower energies but a negative contribution at higher energies. That is, the optical-limit approximation *underestimates* the reaction cross section below $E=200$ MeV but *overestimates* it above 200 MeV. The overestimation by the optical-limit approximation has been emphasized by several authors [19–21], but our statement here is more general. This behavior is determined by the sign of $1 - |e^{i\chi_{\text{DPP}}(2n)}|^2$. Whether $|e^{i\chi_{\text{DPP}}(2n)}|^2$ is

TABLE I. Reaction cross sections of ${}^6\text{He}$ incident on ${}^{12}\text{C}$ in units of mb. E is the bombarding energy per nucleon. σ_{if} corresponds to the last term of Eq. (7). The calculated reaction cross section for ${}^4\text{He}+{}^{12}\text{C}$ at $E=800$ MeV is 516 mb. The measured interaction cross sections at $E=790$ MeV are 722 ± 6 and 503 ± 5 mb for ${}^6\text{He}$ and ${}^4\text{He}$, respectively [18].

E (MeV)	σ_{R}	σ_{f}	$\sigma_{\text{DPP}}(2n)$	$\sigma_{\text{DPP}}({}^4\text{He})$	σ_{if}
50	1279	1193	+84	+6.0	-4.0
100	955	906	+48	+1.0	-0.5
200	686	700	-11	-3.0	-0.1
400	708	766	-52	-5.0	-1.4
800	737	811	-71	-0.7	-2.1

less than 1 or not depends on the sign of the imaginary part of the $2n$ -DPP. As discussed later, it becomes negative at lower energies, so $1-|e^{i\chi_{\text{DPP}}(2n)}|^2$ becomes positive, whereas the situation turns out to be opposite at higher energies.

Before discussing the DPP, we compare the σ_{R} value at $E=800$ MeV to that calculated by a full Glauber model. We repeated the calculation of Ref. [16] using the parameters of the nucleon-nucleon profile function averaged by the proton and the neutron. The wave function of ${}^{12}\text{C}$ was given by a microscopic 3α -cluster model. The σ_{R} values obtained by this fully microscopic calculation are 743 and 509 mb for ${}^6\text{He}+{}^{12}\text{C}$ and ${}^4\text{He}+{}^{12}\text{C}$, respectively, in a good agreement with those listed in Table I. This confirms the soundness of the present approach.

Though the ${}^4\text{He}$ -DPP term has a negligible contribution to σ_{R} , it may not necessarily mean that the core excitation plays no active role, but simply mean that the reaction cross section does not reflect the DPP at short distances. As Eq. (7) shows, the reaction probability for the ${}^4\text{He}$ -DPP term is multiplied by P_{f} , which is almost zero for such a geometry that ${}^6\text{He}$ and ${}^{12}\text{C}$ strongly overlap. Figure 2 displays the imaginary part of the DPP of ${}^6\text{He}$ (solid line) and of ${}^4\text{He}$ (dashed line), respectively. The difference between them is the $2n$ -DPP due to the halo-neutron excitation. Two characteristic points are noted: One is that the DPP of ${}^6\text{He}$ is stronger

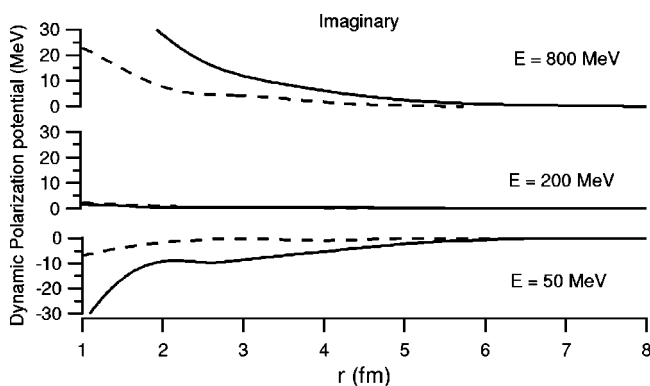


FIG. 2. The imaginary parts of the dynamic polarization potentials for ${}^6\text{He}$ and ${}^4\text{He}$ incident on ${}^{12}\text{C}$. E is the bombarding energy per nucleon. The solid line is for ${}^6\text{He}$ and the dotted line for ${}^4\text{He}$. The difference between them is the polarization potential due to the excitation of halo neutrons in ${}^6\text{He}$.

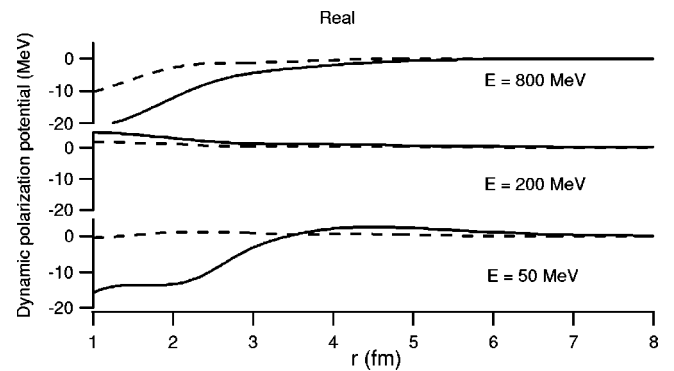


FIG. 3. The same as Fig. 2 but for the real parts.

than that of ${}^4\text{He}$ and has a longer range for all the energies considered here. The latter feature is related to the halo structure of ${}^6\text{He}$. The effect of the halo-neutron excitation to the $2n$ -DPP is quite large at 50 and 800 MeV. Another remarkable point is the energy-dependence of the DPP. The magnitude of both the ${}^6\text{He}$ and ${}^4\text{He}$ DPPs becomes smallest at $E \sim 200$ MeV, which is understood from the fact that the transparency of the p - ${}^{12}\text{C}$ interaction reaches its maximum around that energy [22]. The imaginary part of the DPP is negative below 200 MeV, but turns out to be positive above 200 MeV. The relationship between V_{NT} and the sign of the DPP, stated below Eq. (6), well explains this energy dependence. Figure 3 shows the real part of the DPP. The two characteristic points mentioned above for the imaginary part apply to the real part as well. The sign change of the real part of the DPP is also understood from the rule except for the potential near the origin at lower energies.

The elastic differential cross section of ${}^6\text{He}+{}^{12}\text{C}$ is shown in Fig. 4 at $E=40$ and 400 MeV. The solid line represents the cross section calculated with the full phase $\chi({}^6\text{He})$, the dotted line the cross section calculated by turning off the halo-neutron excitation, namely, with the phase $\chi_{\text{f}}({}^6\text{He}) + \chi_{\text{DPP}}({}^4\text{He})$, and the dashed line the one obtained by neglect-

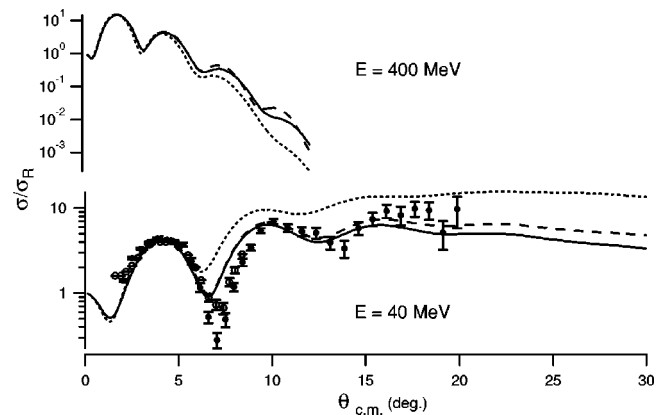


FIG. 4. The elastic differential cross sections in Rutherford ratio for ${}^6\text{He}+{}^{12}\text{C}$ scattering. The p - ${}^{12}\text{C}$ optical potential is taken from Ref. [23] for 40 MeV/nucleon or from Ref. [10] for 400 MeV/nucleon. The phase-shift function used in $\chi({}^6\text{He})$ (solid line), $\chi_{\text{f}}({}^6\text{He}) + \chi_{\text{DPP}}(2n)$ (dashed line), or $\chi_{\text{f}}({}^6\text{He}) + \chi_{\text{DPP}}({}^4\text{He})$ (dotted line), respectively. The experimental data are taken from Ref. [6].

ing the core excitation, i.e., with the phase $\chi_f(^6\text{He}) + \chi_{\text{DPP}}(2n)$. The calculation reproduces the experimental data reasonably well. The effect of including the DPP reduces the cross section at 40 MeV, while the $2n$ -DPP enhances the cross section at 400 MeV because it has a positive imaginary part. Comparing the relative importance of the two DPPs, we see that the halo-neutron excitation generally gives stronger effects than the ^4He -core excitation. The core excitation process nevertheless becomes significant at larger angles; even at 40 MeV, to neglect the core excitation results in 20–40% overestimation of the cross section at the angle of 20° – 30° .

In conclusion we have studied the dynamic polarization potential due to the nuclear excitation for a halo nucleus ^6He incident on ^{12}C at medium energies. Both the halo-neutron and the core-nucleon excitations are taken into account by using the realistic wave function generated from a variational Monte Carlo calculation. The polarization potential has been calculated from the nucleon-target optical potential in the eikonal approximation. We find that the imaginary part of the

polarization potential changes a sign (negative to positive with increasing energy) around 200 MeV/nucleon. Because of this energy-dependence the optical potential of ^6He tends to be more absorptive than the folded potential at lower energies but less absorptive at higher energies. Thus the optical-limit approximation underestimates the reaction cross section at lower energies but overestimates it at higher energies. The real part of the polarization potential also changes a sign at least near the surface; repulsive to attractive around 300 MeV/nucleon. The effect of the halo-neutron excitation is larger than that of the ^4He core excitation but the latter still gives a significant contribution to the elastic differential cross section at large angles.

One of the authors (B.A-I.) is supported financially by JSPS (the Japan Society for the Promotion of Science) for Foreign Researchers (No. P03023). This work was in part supported by JSPS Grants-in-Aid for Scientific Research (Nos. 14540249 and 15003023).

-
- [1] H. Feshbach, *Ann. Phys. (N.Y.)* **19**, 287 (1962).
 [2] G. R. Satchler and W. G. Love, *Phys. Rep.* **55**, 183 (1979); M. E. Brandan and G. R. Satchler, *ibid.* **285**, 143 (1997).
 [3] Y. Sakuragi, M. Yahiro, and M. Kamimura, *Prog. Theor. Phys. Suppl.* **89**, 136 (1986).
 [4] M. V. Andrés and J. Gómez-Camacho, *Phys. Rev. Lett.* **82**, 1387 (1999).
 [5] K. Rusek, N. Keeley, K. W. Kemper, and R. Raabe, *Phys. Rev. C* **67**, 041604(R) (2003).
 [6] V. Lapoux *et al.*, *Phys. Rev. C* **66**, 034608 (2002).
 [7] B. Abu-Ibrahim and Y. Suzuki, *Phys. Rev. C* **61**, 051601(R) (2000); *Nucl. Phys.* **A728**, 111 (2002).
 [8] B. Abu-Ibrahim and Y. Suzuki, *Nucl. Phys.* **A728**, 118 (2003); **A732**, 218 (2004).
 [9] B. S. Pudliner, V. R. Pandharipande, J. Carlson, S. C. Pieper, and R. B. Wiringa, *Phys. Rev. C* **56**, 1720 (1997).
 [10] E. D. Cooper, S. Hama, B. C. Clark, and R. L. Mercer, *Phys. Rev. C* **47**, 297 (1993).
 [11] R. J. Glauber, in *Lectures on Theoretical Physics*, edited by W. E. Brittin and L. C. Dunham (Interscience, New York, 1959), Vol. 1, p. 315.
 [12] R. S. Mackintosh and K. Rusek, *Phys. Rev. C* **67**, 034607 (2003).
 [13] L. F. Canto, R. Donangelo, and M. S. Hussein, *Nucl. Phys.* **A529**, 243 (1991).
 [14] K. Yabana, Y. Ogawa, and Y. Suzuki, *Phys. Rev. C* **45**, 2909 (1992).
 [15] H. Esbensen and G. F. Bertsch, *Phys. Rev. C* **64**, 014608 (2001).
 [16] K. Varga, S. C. Pieper, Y. Suzuki, and R. B. Wiringa, *Phys. Rev. C* **66**, 034611 (2002).
 [17] K. Arai, Y. Suzuki, and R. G. Lovas, *Phys. Rev. C* **59**, 1432 (1999).
 [18] I. Tanihata *et al.*, *Phys. Lett.* **160B**, 380 (1985).
 [19] Y. Ogawa, K. Yabana, and Y. Suzuki, *Nucl. Phys.* **A543**, 722 (1992).
 [20] J. S. Al-Khalili and J. A. Tostevin, *Phys. Rev. Lett.* **76**, 3903 (1996).
 [21] R. C. Johnson and C. J. Goebel, *Phys. Rev. C* **62**, 027603 (2000).
 [22] R. M. DeVries and J. C. Peng, *Phys. Rev. Lett.* **43**, 1373 (1979).
 [23] J. Rapaport, *Phys. Rep.* **87**, 25 (1982).